Powder Technology 245 (2013) 13–20

Contents lists available at SciVerse ScienceDirect

Powder Technology

journal homepage: www.elsevier.com/locate/powtec

Liquid phase densification of Al-4.5 wt.% Cu powder reinforced with 5 wt.% Saffil short fibers during hot pressing

M.F. Moreno *, C.J.R. González Oliver

Centro Atómico Bariloche, Av. E. Bustillo 9500, (8400) S.C. de Bariloche (RN), R., Argentina
C.O.N.IC.E.T. Av. Rivadavia 1917, Capital Federal, R., Argentina

ARTICLE INFO

Article history:
Received 1 April 2011
Received in revised form 2 November 2012
Accepted 16 January 2013
Available online 23 January 2013

Keywords:
Hot pressing
Metal matrix composites
Ceramic short fibers
Liquid phase sintering
Power Law Creep
Super plastic deformation

ABSTRACT

The Alumix 13 (wt.%) (Al–4.5 Cu 0.5 Mg 0.2 Si) powder with and without 5 wt.% Saffil short fibers specimens were hot pressed in the range 580–620 °C. The densification during pressure increase was fitted using the Konopicky model and an agreement with the associated linear plot P vs. $\ln(1/(1-D))$ was found for both materials, where P is applied pressure and D is the relative density of the porous material.

The transient liquid phase formed from the elemental Al and Cu powder particles above the eutectic temperature of 548 °C at low hot pressing pressures, allows to increase the densification due to the reduction in the yield stress of the porous material. The active liquid flow enhanced the deformation between Al particles in the beginning of the pressure ramp.

For higher pressures, a sudden break to a higher slope in Konopicky plot was found. This hardening behavior was detected from 610 °C for pure Alumix 13 and it was systematically developed at 580, 600, 610 and 620 °C for the composites, and it can be assigned to diffusion of Cu into the Al grains.

During the constant pressure stage the densification was well fitted using the Power Law Creep model with exponents of $n=1$ and $n=2$, which are related to Newtonian viscous flow and superplastic deformation, respectively. Besides, final hot pressed composites samples retained an important quantity of solidified liquid phase located in between the Saffil fibers agglomerates.

1. Introduction

An amorphous or crystalline oxide layer is always present on aluminum surface powder particles due to its high negative enthalpy of oxide formation [1]. This thermodynamically stable ceramic layer prevents any solid state sintering between Al particles [2]. One way to reduce that contamination is by chemical reaction considering that Mg is an element that reduces Al oxide [$1.5\,Mg + 2Al_2O_3 \rightarrow 1.5MgAl_2O_4 + Al$], therefore the spinel $MgO.Al_2O_3$ can be produced from that reaction [3]. When the powder is pressed at high pressures (during cold pressing for instance), due to cold plastic deformation, the oxide layers can be fracture providing an interlocking of the Al particles. If the temperature of the pressed Al powder with Cu particles is raised, over the eutectic binary Al–Cu system temperature $T_{EU} = 548$ °C (during sintering for instance), then both metals react forming a transitory liquid phase [3,4]. The eutectic liquid formed between Al and $CuAl_2$ enhances the sintering and welding of Al particles, but not necessarily the porous material increases its density [4]. Some attempts, such as adding trace elements, to improve the wettability between Al–Cu liquid and Al_2O_3 were studied [5,6] but no significant changes were obtained in wetting angles [5]. During Al–Cu sintering at $T > T_{EU}$ another important process is observed: the Cu diffusion from the liquid into Al grains in short times [3]. Those processes related to Al–Cu liquid phase during hot pressing [7] are further studied in this work for a commercial mixture powder (Alumix 13), which contains (wt.%) Al–4.5 Cu 0.5 Mg and 0.2 Si. Additionally a 5 wt.% Saffil alumina short fibers were used to reinforce the powder matrix.

Earlier works [7–9] have shown that Konopicky model, based on the micromechanical model developed by Torre [10], can adequately describe the densification behaviors for both temperature ranges: during cold [8] and hot pressing.

$$kP = \ln[1/(1-D)] + B_{MK} \quad (1)$$

where D, is the relative density (dimensionless) obtained as the ratio: ρ instantaneous/ρ theoretical, B_{MK} is a constant depending on D_0 (initial relative density) and k is equal to $3/(2\sigma_{YS})$. Therefore, σ_{YS} (is the yield stress of the whole material, agglomerates and pores) can be calculated from this linear plot P vs. $\ln(1/(1-D))$, henceforth be called 'Konopicky plot'. Such agreements with the model were obtained for a wide range of powder compositions based on pure Al, rapid-solidification Al alloy [7] and Alumix 13 including composites reinforced with Saffil fibers [7–9]. It is common to find in the open literature, many studies related to aluminum

* Corresponding author at: C.O.N.IC.E.T. Av. Rivadavia 1917, Capital Federal, R., Argentina.
E-mail address: mmoreno@cab.cnea.gov.ar (M.F. Moreno).

0032-5910/$ – see front matter © 2013 Elsevier B.V. All rights reserved.
http://dx.doi.org/10.1016/j.powtec.2013.01.026

powder metallurgy synthesis, including hot pressing, where ceramic particles [11] or whiskers were used as reinforcements, but only few works are concerned to the use of short fibers [6,7,9,12].

In references [12,13] it was considered that the hot pressed pure and SiC short fibers reinforced Al powder over 350 °C deforms under Power Law Creep mechanism, approximated as:

$$\dot{\varepsilon} = A_0 \sigma^n \tag{2}$$

where $\dot{\varepsilon}$ is the strain rate, A_0 is a microstructural constant depending on temperature and the material, σ can be taken as an effective stress and n is the stress exponent, which represents the deformation mechanism. It is considered the plastic material deforms under creep conditions due to the temperatures and pressures applied to the whole material (aluminum particles, pores and ceramic fibers).

For the final stage of closed porosity ($D > 0.9$) the densification at constant pressure and temperature can be fitted by the Power Law Creep mechanism [7,12–14]. Then the densification rate can be expressed as a function of D and n as

$$dD/dt = (3A_0/2)\left\{\left(D(1-D)/\left[1-(1-D)^{1/n}\right]^n\right\}(3P_e/2n)^n. \tag{3}$$

The expression $D(1-D)/[1-(1-D)^{1/n}]^n$ decreases with an increasing D, during densification. It was found this model agreed for pure Alumix 13 as well as for Alumix 13–11 wt.% Saffil fibers composite during hot pressing [7,12]. The densification rate can be plotted as a function of $D(1-D)/[1-(1-D)^{1/n}]^n$, for a fixed $P = P_{MAX}$ and the controlling mechanism can be assessed if this plot is linear for a certain n exponent. The value $n = 1$ represents a viscous flow process [15] and $n = 2$ is found for the case of superplastic deformation [16]. The case of $n = 3$ applies to the viscous glide mechanism [17].

In this work the axial hot pressing densification, during the increase in pressure stage as well as during the isobaric and isothermal stage, of pure and reinforced powder materials based on Alumix 13 alloy and Saffil short fibers are further studied using new compositions. The final microstructures were carefully examined and correlated to the processing steps.

2. Experimental

2.1. Materials

The materials were based on Alumix 13 (Eckart-Werke, Germany) powder, a commercial mixture of elemental pure Al particles (95 μm mean diameter) obtained by atomization and 4.5 wt.% of pure Cu dendritic particles. The other alloying elements present are Mg (0.5%) and Si (0.2%). The ceramic reinforcements used were Saffil (Saffil Ltd., UK) short fibers. The fibers were mainly composed by δ−γ-alumina phases with a content 2–3 wt.% of SiO_2 and they were classified having mean diameter of 2–5 μm and lengths of about 50–200 μm. The theoretical densities were 2.78 and 3.3 g cm^{-3} for Alumix 13 and Saffil fibers respectively. The rule of mixture was used to calculate the density of 2.8 g cm^{-3} for the composite material. The composite was obtained by mixing Alumix 13 with 5 wt.% Saffil fibers in ethyl alcohol with a mechanical stirrer and followed by Cole Palmer ultrasonic head mixing. The pure Alumix 13 and composite materials were heated at 200 °C under vacuum to eliminate the original wax content of Alumix 13 (about 1.5 wt.%) after drying in muffle at 80 °C. The Eckart Werke AS081 pure aluminum powder (45 μm mean diameter) is made of 99.5% Al atomized ligamentary shaped particles with the same composition impurities than the Al base powder of Alumix 13.

Additionally, two samples based on AS081 aluminum powder, one of pure AS081 and the other reinforced with 5 wt.% of Saffil short fibers, were hot pressed as references for further comparative densifications under similar conditions than those used for the Alumix-13 hot pressed samples.

2.2. Axial hot pressings

The materials were filled into a high density graphite double action axial die. Boron nitride powder was used to prevent the sticking between the sample and the graphite parts (die and pistons). In similar way as described elsewhere [7,12] the die was located into a vacuum reactor, which was attached to a universal testing machine MTS 810 to apply the compression load to the pistons. The pure Alumix 13 samples noted as A13-x were hot-pressed at 590, 610 and 620 °C (Table 1). The composites samples noted as A13S5-1, 2, 3, and 4 were hot-pressed at 590, 600, 610 and 620 °C respectively. A13S5-1, 2, 3 were unloaded, heated up to 620 °C and repressed up to about 22.1 MPa.

The pure aluminum AS081 sample and AS081-5 wt.% Saffil composite were hot pressed at 630 °C using the same devices configuration (Table 1). Two densification stages were recorded during hot pressing: i) a ramp of pressure where ΔP/t was the pressure rate until P_{MAX} was reached; and ii) a constant load period stage, characterized by a period of time while the load was maintained constant (after the ramp of pressure stage). The D_{RP} values in Table 1 were the maximum relative densities reached at P_{MAX}.

Density ρ of each sample was calculated from the final mass and geometric dimensions, accuracies of the scale and micrometer were 1 mg and 10 μm respectively. Due to the constancy of the diameter and mass, the reduction of instantaneous thickness sample (height) is inversely related to the increase in density. The relative density $D = \rho/\rho_{full\ density}$ during hot pressing was calculated using the density of each material and the rule of mixtures [7].

The initial aspect ratios L_0/ϕ (height/diameter) were about 0.26 to 0.28 to ensure more homogeneous pressure distribution into the cylindrical sample [12]. The temperature and vacuum were stabilized during 1 h before each hot pressing cycle. No flooding of the system with N_2 was done before pressing as effected in reference [7]. Also in this work an ultrasonic tip was used for a better mixing of the fibers with the powder.

2.3. Quenching and sintering experiments

A single pellet made of pure Alumix 13 was pressed until relative density D ~ 0.84. Smaller specimens were extracted from that green pellet by cutting plates of 4 mm × 2 mm with 1 mm thickness. Two quenching experiments (QC) were carried out after heating at 577 and 630 °C during 5 min under Ar flow. Then, the samples were cooled directly by immersion into ice cooled water.

Finally, a cold compacted green pellet composed by Alumix 13–5 wt.% Saffil fibers with relative density of 0.95 was sintered by

Table 1
Parameters of hot pressings.

Sample	Composition powder/wt.% fibers	Temp. [°C]	ΔP/t [MPa/s]	P_{MAX} [MPa]	Constant pressure time [min]	D_{RP}
A13-1	100 Alumix 13	580	0.58	22.0	70	0.99
A13-2	100 Alumix 13	600	0.58	21.8	32	0.99
A13-3	100 Alumix 13	610	0.14	20.3	69	0.97
A13S5-1	Alumix 13/5 Saffil	580	0.58	22.1	32	0.85
		620	0.58	22.1	45	0.97
A13S5-2	Alumix 13/5 Saffil	600	0.58	22.1	39	0.85
		620	0.58	22.1	50	0.95
A13S5-3	Alumix 13/5 Saffil	610	0.58	22.1	40	0.91
		620	0.58	22.1	60	0.96
A13S5-4	Alumix 13/5 Saffil	620	0.58	20.2	105	0.91
AS081	100 Al AS081	630	0.14	15.14	26	0.94
AS081-5% Saffil	Al AS081/5 Saffil	630	0.14	15.13	73	0.81

heating up to 620 °C in a differential dilatometer (Theta Dilatronics, USA) under N_2 flow. Both, sintering and quenching experiments were parts of some extensive studies related on Alumix 13/Saffil fibers composites sintering [12].

2.4. Microstructural characterization

Hot pressed, quenched and sintered samples were cut and polished along the different compacted orientations to study the final resulting microstructures. Keller reagent was used as metallographic etching. Leyca optical microscope, Philips SEM 515 scanning electron microscope (SEM) and energy dispersion spectrum (EDS-EDAX) were operated at 20 kV to study the different final materials using standard parameters of detection. The X-ray diffractometry (XRD; Philips PW 1700) with Cu-Kα radiation (0.154054 nm) source was used to obtain diffraction patterns of pure Alumix 13 loose powder, mixtures with about 5 wt.% of pure Si powder to calibrate the diffraction angle (2θ). In addition final hot pressed samples were cut and polished to be examined by XRD between 20 and 80º angles (2θ) and dwell time of 1 s before increment of 0.01 degree.

3. Results

3.1. Densification data for the increase in pressure stage

In Fig. 1, the experimental densification curves relative density D vs. pressure P, during hot pressing for both materials at different temperatures are plotted up to P_{MAX} including the constant pressure stage. Taking into account that the fiber volume fraction is about 0.04 its probable incidence in the initial Do was confirmed. The lower composites initial densities (D_0<0.4) are also related to the raising of the porous volume, due to Saffil fibers ability to form clusters and agglomerations during mixing and after drying [8].

Almost full D was obtained for A13-x after the ramp of pressure stages as shown by their D_{RP} values (0.97 -0.99) in Table 1. Thus in Fig. 1, the densification during constant pressure stage is negligible for unreinforced samples or matrices. For the composites the D_{RP} values were lower than for pure Alumix 13 (Table 1) as it is shown in Fig. 1, by the vertical points at constant P, also denoting the significant densification obtained during this step.

As it was mentioned above, the linear fitting of Konopicky model can be used to calculate the yield stress of a plastic porous material during the ramp of pressure stage. Earlier work [7] has shown that after Konopicky fittings in terms of P vs. ln [1/(1 − D)] at 606 °C for pure Alumix 13, two slopes were obtained. A straight line fitted well with the experimental points for lower pressures until a sudden slope increase (or break at $P = P_C$) at higher pressure was met. A second and higher slope straight line fitted the rest of the points at pressures higher than P_C. The same behavior of changing slope could be obtained at 611 °C on Alumix 13–11 wt.% Saffil composite [7]. However, in this work the behavior of changing slope could be slightly detected at 600 °C for hot pressed pure Alumix 13 and the Konopicky plot at 580 °C was a straight line (open circle points in Fig. 2). For hot pressing at 610 °C (A13-3) the behavior of changing slope became more evident. The pressure P_C can be defined in a Konopicky plot, by extrapolating both linear fittings up to their intersection. In Fig. 2 both linear fittings (lower and higher slopes) are plotted and extended to obtain P_C for A13-3 and in Table 2 the parameters are listed.

4. Discussion

4.1. Final microstructures

The microstructures of A13-x hot pressed samples can be seen in Fig. 3a (580 °C, Al3-1) and b (600 °C, Al3 − 2) both corresponding to planes parallel to the pressing axis. Using the same metallographic preparation and magnification a difference in the liquid phase spreading can be observed and it could be assigned to the different hot-pressing temperatures, and the lower apparent porosity for A13-2. A13-1 and A13-3 formed quite a dispersion of solidified phase with a high level of Cu (74.1 wt.% Al, 24.9%Cu, 0.95%Mg). That dispersion was found mainly at the joints of aluminum boundaries (white phases in Fig. 3a) as a common microstructural feature. On the other hand, a fine and uniform liquid spreading along the boundaries was found in A13-2. Similar semi-continuous network through Al particles boundaries was found in 25 μm Al particles/5% Cu hot pressed at $P_{MAX} = 25$ MPa and 600 °C, for only 5 min [11].

A fine structure formed in the centre of grains in A13-1 and A13-3 (610 °C, Fig. 3c) but not in A13-2. This plate-like structure was analyzed by EDS giving a Cu content 6% lower than that for the intermetallic theta ($CuAl_2$; 54 wt.%Cu–46%Al). It must be noted that their thicknesses of about 100–200 nm (detected by SEM, Fig. 3c) were thinner than 1 μm EDS window, which increases artificially the Al content from the Al matrix background; therefore, the composition of the plates is approaching that for $CuAl_2$ [18]. Transmission electron microscopy should be needed to confirm accurately that phase. The surrounding zone to those plates corresponds to Al with less than 2% of Cu content, due to the out-diffusion of Cu from the liquid before the solidification process [3].

The fibers adopted two different arrays within the Alumix 13 matrix. First are fiber-agglomerates. The second 'fibers array' belongs to the poorly-reinforced zones characterized by a low volume fraction

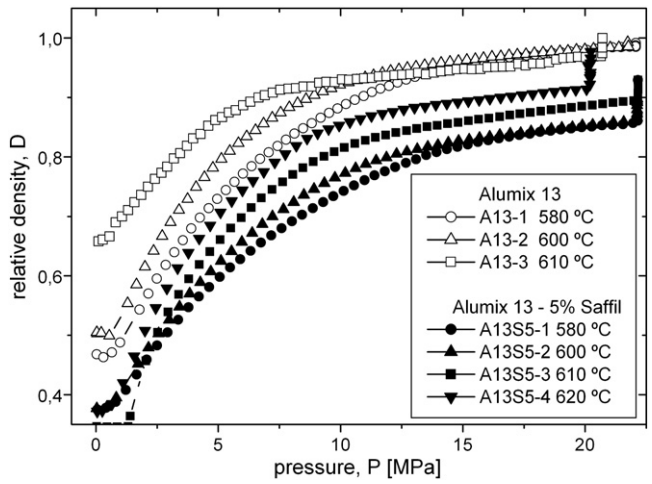

Fig. 1. Hot pressing densification curves for pure Alumix 13 and composites materials.

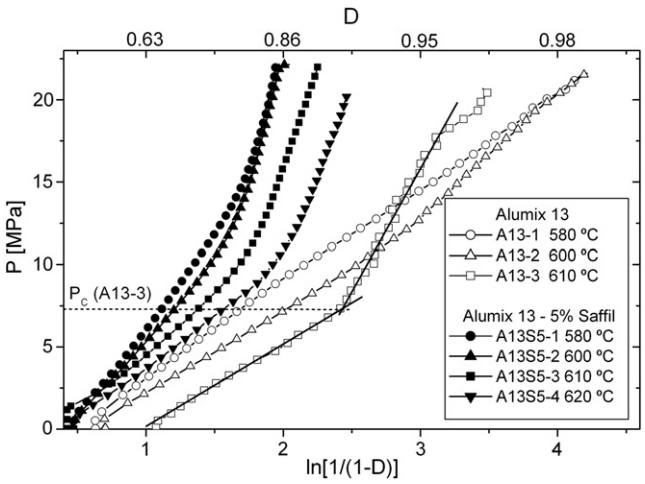

Fig. 2. Konopicky plots for pure Alumix 13 and composites materials.

Table 2
Parameters and results from Konopicky fittings. σ_{YSI} and σ_{YSF} mean yield stresses before and after P_C respectively [7]. Results from previous work.

Sample	Composition powder/wt.% fibers	Temp. [°C]	Pressure range fitting [MPa]	σ_{YS} [MPa]	P_C [MPa]	$\sigma_{YSI}/\sigma_{YSF}$
A13-1	100 Alumix 13	580	0.6–22	8.6	–	1
A13-2	100 Alumix 13	600	0.6–10.7	7.6 (σ_{YSI})	10.7	1.45
			11.8–19.4	11.0 (σ_{YSF})		
A13-3	100 Alumix 13	610	1.4–7.1	7.44 (σ_{YSI})		
			9–18.5	22.5 (σ_{YSF})	7.3	3.0
Alumix 13 [7]	100 Alumix 13	606	7.5–12	14.49 (σ_{YSI})	13.5	1.8
			12–25	26.24 (σ_{YSF})		
AS081	100 Al AS081	630	0–8	13.1 (σ_{YSI})	–	–
			8–15	8.7 (σ_{YSF})		
A13S5-1	Alumix 13/5 Saffil	580	1.3–12.5	16.3(σ_{YSI})	14.4	3.1
			17.3–22	50.0 (σ_{YSF})		
A13S5-2	Alumix 13/5 Saffil	600	2–9.5	14.2 (σ_{YSI})	11.5	3.4
			14.5–21.7	48.8 (σ_{YSF})		
A13S5-3	Alumix 13/5 Saffil	610	2.7–8	10.9 (σ_{YSI})	10	3.3
			12.5–22	35.9 (σ_{YF})		
A13S5-4	Alumix 13/5 Saffil	620	1.1–8.7	9.3 (σ_{YSI})	10	3.5
			12.5–20	33.0 (σ_{YSF})		
Alumix 13–11 wt.% Saffil [7]	Alumix 13/11 Saffil	611	6–12.5	10.17 (σ_{YSI})	14	2.35
			15–24	23.96 (σ_{YF})		
AS081-5% Saffil	Al AS081/5 Saffil	630	0–15	18.8	–	–

of fibers. The main feature of clustered fibers was the alignment of their axes along planes perpendicular to the pressing axis and having random directions within the plane. This kind of fiber-distribution is often found in axial hot pressed samples due to face pistons movement [7,9]. Fig. 4a (OM micrograph) shows the plane image where many fibers are located randomly. Fig. 4b shows a cross section of an agglomerate where many fibers are perpendicular to the vertical pressing direction. Also, it was found a minor quantity of fibers in the transverse direction. The fibers in the poorly-reinforced zone have non preferential direction. A deeper EDS analysis revealed that these clustered fiber structures retained Cu-rich phases after the final hot pressing cycles. In addition, within those fiber clustered zones porosity was clearly detected; which agrees with the final relative density for the hot pressed composites ($D_F<1$). Fig. 4c shows the same liquid segregated structure (white phases) found in A13-1 and A13-3 samples along the grain boundaries and around the short fibers. Other common microstructural feature was the plate-like phase (similar to $CuAl_2$ [18]) in the centre of the grains similar to that found for A13-1 and A13-3. This coarse structure is related to a long period of time at $T>T_{EU}$ and to high pressure during constant pressure stage (Table 1).

4.2. Liquid phase spreading

The rapid spreading effects were clearly detected in the QC experiments. Fig. 5a shows that a fine liquid phase spreading is obtained in the pellet quenched from 577 °C. Fig. 5b shows the same pellet quenched from 630 °C where the liquid phase became thicker than that for 577 °C, showing also a clear tendency to migrate inside the Al grain. For both samples the liquid phase is located as a thin layer between the Al grains and a kind of 'branches' (label '1' in Fig. 5a and b) that squeeze inwards to the centre of grains. Also the white rounded phase was analyzed (label '3' in Fig. 5a and b) resulting with 73% Al, 24% Cu, 0.3% Mg and 2% Fe.

Fig. 6a shows the pressureless sintered (using a dilatometer) sample of Alumix 13–5 wt.% Saffil composite where a portion of Cu (white phase labelled as Cu) still remains pure between Saffil fibers ('f' in Fig. 6a). The zone labelled as '3' was in contact with Al particles and formed a phase having 67% Al- 33% Cu- 1% Mg average composition and in the centre of the aluminum grain (label '4' in Fig. 6a) gave 1.4% Cu, 98.6% of Al. Close to Cu some pores are found in the sintered sample, between the ceramic fibers. The porosity generation that reduces the density is associated to liquid phase sintering process called swelling, typically found in Al–Cu powders sintering and is associated to the formation of liquid in Al–Cu contacts and subsequent spreading of the liquid into the body [12,19,20]. It is noted the ceramic fibers retain Cu dendrites during the cold pressing and after further sintering, a portion of the formed liquid phase was encapsulated or surrounded by fibers. It was found the same process of liquid formation operates in the composites samples during hot pressing. The final structure of hot pressed A13S5-3 showed zones with liquid phase (solidified) retained between the Saffil fibers. The insert, in Fig. 6b represents a backscattered electron-image where the Cu content contrast is evident. The average wt.% composition of these zones

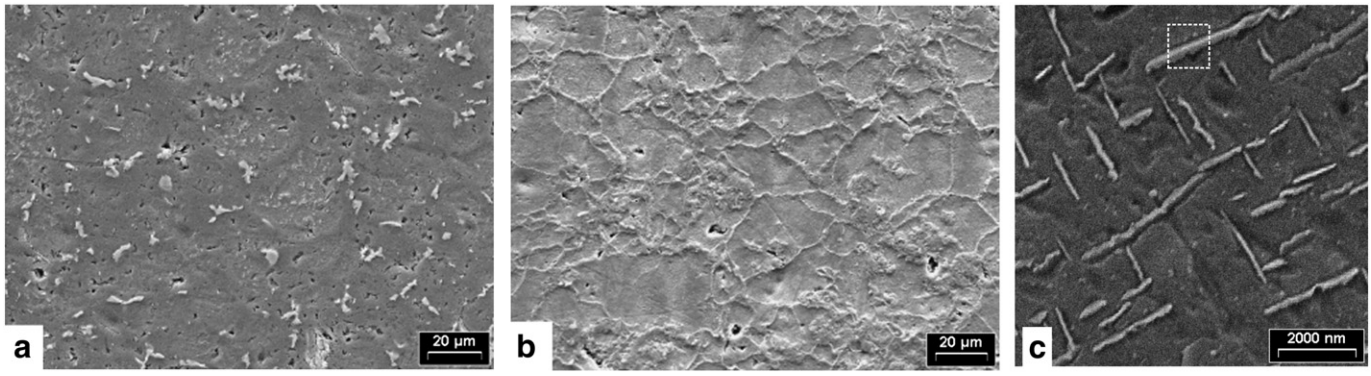

Fig. 3. SEM images of hot pressed samples a) A13-1, b) A13-2 and c) A13-3(dotted line is the EDS probing window).

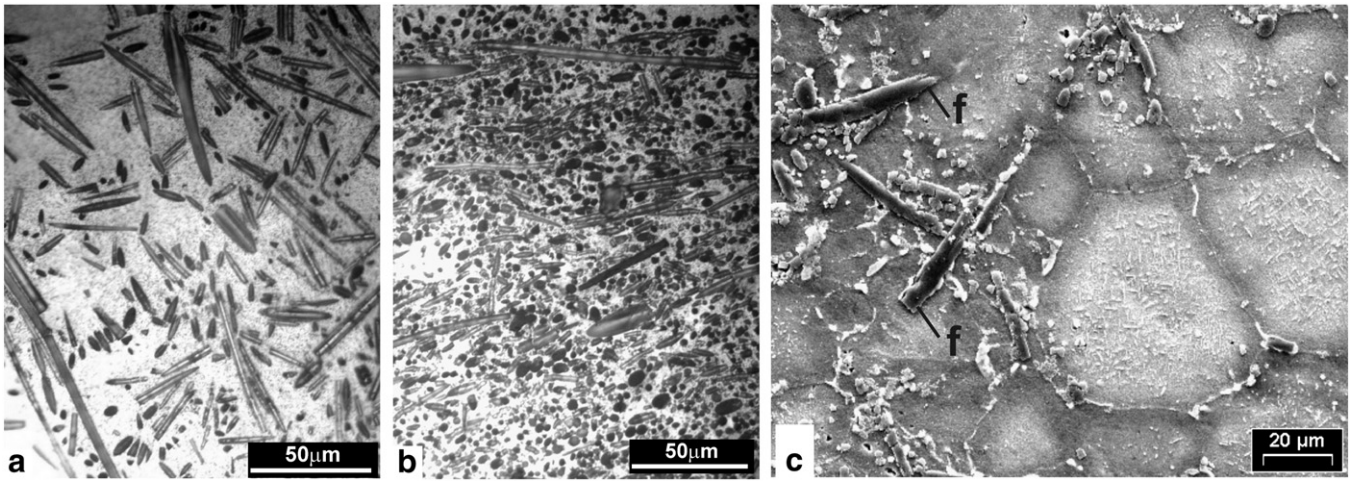

Fig. 4. Hot pressed A13S5-1 sample a) and b) Optical micrographs c) SEM image, "f" are Saffil fibers.

is about 75% Al–33% Cu–2% Mg. It should be noted the obvious differences in the pore structure and the final grain morphology between sintered (including QC) samples and hot pressed samples. Due to the high plasticity of the Al grains and the external pressure, only a few percent of porosity remains in the hot pressed specimens (label '1' in Fig. 5c). Therefore, no swelling could be developed during hot pressing.

On the other hand, for the sintered and QC samples two kinds of porous structures were observed: i) the trapped pores due to encapsulation by plastic deformation during cold pressing (label '5' in Fig. 5a) and ii) the pores initially occupied by Cu dendrites that are consumed when liquid is formed and flow away at a later stage (label '4' in Fig. 5b).

In the QC samples the inner zone of grains indicated that Cu diffused into the Al matrix, increasing the Cu content from 1 to 2.3 wt.% Considering the relative short time (about 5 min) exposed at $T > T_{EU}$ the fast Cu diffusivity in Al is clear (around 5000 times faster than for Al in Cu [3]). Therefore, at least two important phenomena are controlling the pressureless densification and they can help to explain the behavior of changing slope in the hot pressing of Alumix 13 materials: i) the high reactivity between Al and Cu, enhanced by the presence of 0.5% Mg, due to improvement of the Al sintering [4]; and ii) the high Cu diffusivity into Al to form the solid solution. The liquid phase is thus formed at the beginning of the pressing when the Cu dendrites react with the Al particles (also enhanced by the increase in contact pressure) spreading out around the surface of the neighbouring particles.

The final compacted grain structure of pure Al-AS081 hot pressed sample can be seen in Fig. 7c in the SEM micrograph. The white lines are the etched grain boundaries but no evidence of liquid phase was found at all. At hot pressing temperature of 630 °C only plastic yielding and creep are the only possible mechanisms to deform the pure Al powder particles and increase its densification [12].

Other consequence of the Saffil fibers tendency to agglomerate is that during the hot pressing the fiber-fiber contacts are formed. However, no damage or fractures could be detected in the final materials, as already noted in [13] for SiC fibers after similar hot pressings. That is important when the aspect ratio of reinforcement must be maintained.

The same structure of orthogonal plate-like phase was found in the inner zones of the grains of the four composites. The optical micrograph of Fig. 7a shows that the discontinuous segregated liquid areas (rounded grey phases in the grain boundaries) were similar to those found in Fig. 3a for the A13-1 sample. The same orthogonal plate-like morphology as that found in pure Alumix 13 samples A13-1 and A13-3 (Fig. 3c) was found in A13S5-1. The constant pressure period of time (see Table 1) for A13-2 was roughly half the time for the other specimens and this can be the reason why A13-2 did not show the above plate morphology. Therefore, the overexposure to P_{MAX} is related to the formation of this inner coarse orthogonal plates structure.

XRD analyses were recorded (Fig. 8) for pure Alumix 13 powder, doped with pure Si powder for pattern reference, A13-x samples

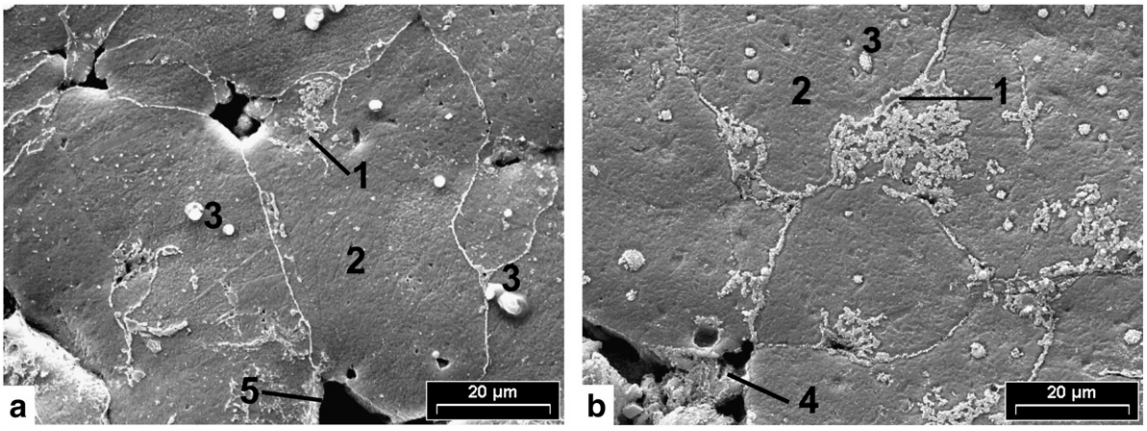

Fig. 5. Pure Alumix 13 QC samples from a) 577 °C and b) 630 °C.

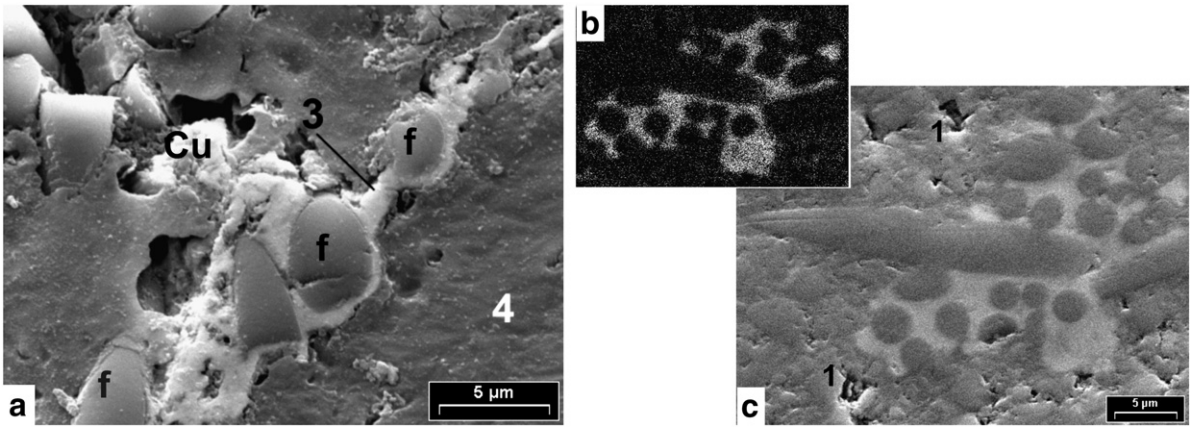

Fig. 6. Alumix 13–5 wt.% Saffil pressureless sintered sample. b) backscattered electrons image of A13S5-3 hot pressed sample, c) SEM image of b).

and the composite A13S5-1. The XRD results reveal the presence of $CuAl_2$ theta phase peaks for long-times constant pressure stage samples, that was for A13-1, A13-3 and A13S5-1 but no clear evidence of that intermetallic phase in A13-2 was detected.

4.3. Densification at constant pressure

As explained above the exponent of $n=2$ was selected to plot dD/dt vs.

$D(1-D)/[1-(1-D)^{1/n}]^n$ and in Fig. 9 it is noted acceptable linear straight fits were found for all cases.

It is mentioned Koike, Mabuchi and Higashi [21] observed by TEM *in-situ* the formation of a liquid phase at 510 °C in a MMC based on 2124 AlCuMg alloy/Si_3N_4 whiskers reinforced. That material was made previously by hot pressing and they found that the partial melting of grain boundaries allowed a better deformation of the whole material. The fraction of liquid phase improved both grains rotation and particle migration; which are the main mechanisms for superplastic deformation.

As it was considered in the Introduction section, the possibility to use $n=1$ and $n=3$ was considered, thus both exponents were replaced in Eq. (3) for the highest hot pressing temperature, of 620 °C, for the composites. These plots are shown together with the $n=2$ Power Law Creep plots in Fig. 9 and the curvature obtained for $n=3$ (continuous line) is clear, meanwhile there is a good agreement for $n=1$ (hollow circle points), *better* than for $n=2$. The $n=1$ exponent is representative for a Newtonian flow deformation considering the possible existence of retained liquid phase; therefore this exponent can suggest that mechanism. It must be pointed out that the range of dD/dt for which linear fittings were obtained in the present work, is much larger than the previous fitting range in reference [7].

Fittings with $n=1$ and $n=3$ were also performed for the other lower temperatures of 610, 600 and 580 °C, and there was a lack of linearity. Therefore, the two possible mechanisms that control the final densification under constant P and temperature are viscous flow ($n=1$) and superplasticity $n=2$. When $n=1$ is inserted in Eq. (3) it results in the following viscous flow expression (similar to that for the hot pressing of glassy grains)

$$dD/dt \sim (P/3\eta)(1-D) \tag{4}$$

where η is the viscosity of the assumed liquid like or vitreous material [7]. It is in agreement with the plot made for 620 °C data where a good linear fit was obtained (open circles in Fig. 9). Finally, it must be considered that the Eq. (4) was applied to the whole composite material and further work is needed to model the reduction of plastic volume fraction owing to ~4% of non-deformable ceramic reinforcement. This modification could only modify slightly the slopes listed in Fig. 9.

This is mainly related to the process of hot densification under pressure and the matrices and the related composites are compared using the above plastic-deformation models for porous metallic bodies.

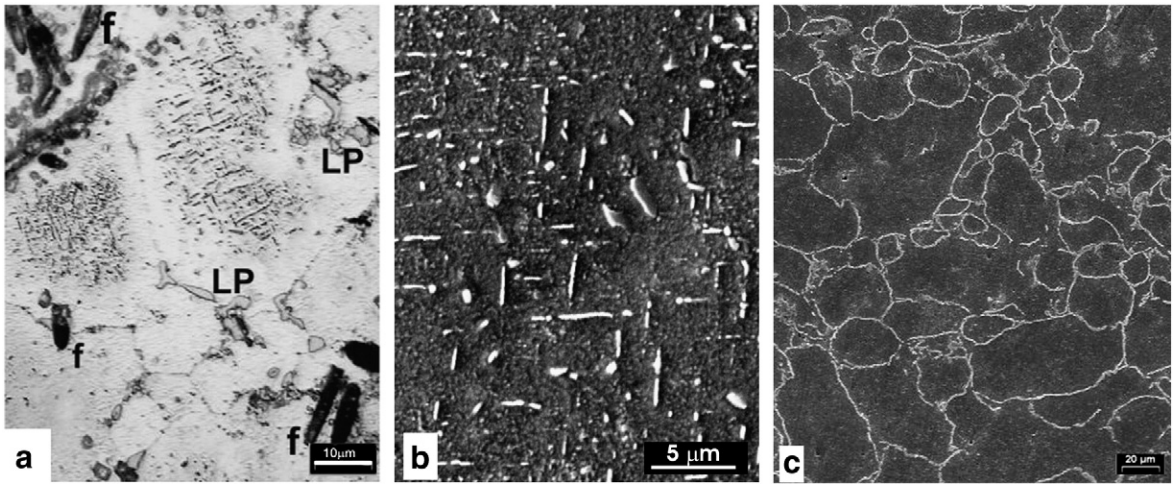

Fig. 7. a) Optical micrograph of A13S5-1. b) SEM image of inner grain A13S5-1. c) SEM image of pure AS081 hot pressed sample.

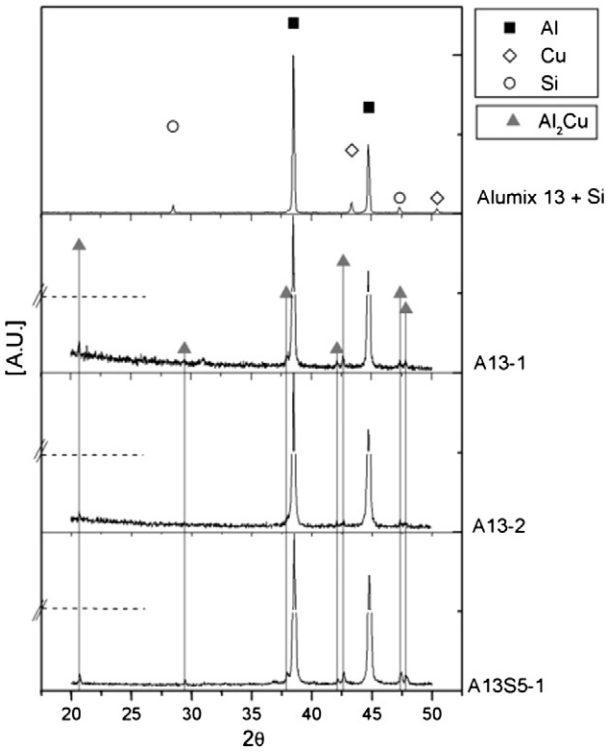

Fig. 8. XRD analysis corresponding to hot pressed samples, using Alumix 13 with pure Si as reference.

4.4. Konopicky behavior

In Table 2 are listed the Konopicky fitting parameters obtained from Fig. 2, P_C values, the yield stress at lower pressures (σ_{YSI}), $P<P_C$, and at higher pressures (σ_{YSF}). The ratio $\sigma_{YSF}/\sigma_{YSI}$ represents the hardening developed by the porous material during its densification. Also the previous results [7] at 606 °C (Alumix 13) and 611 °C (Alumix 13–11% Saffil) were included in Table 2.

During the increase of pressure stage the Konopicky plots, for the four composites, showed also systematically the behavior of changing slope as seen in Fig. 2. It is noted that P_C values (Table 2) decreased with the hot pressing temperature on composites but the hardening ratio was almost constant (3 to 3.5).

When σ_{YSI} values (A13-2/A13-3 and A13S5-2/A13S5-3, Table 2) are compared at 600 and 610 °C it is clear the addition of 5 wt.% of Saffil fibers increases the yield stress of the composites. The extra pressure is needed to deform plastically the particles during the filling of the volume gap or clusters made of fibers. A13-3 sample showed a well defined behavior of changing slope and its $\sigma_{YSF}/\sigma_{YSI}$ ratio is slightly lower than that for the composites. Thus the fibers addition also developed a hardening in composite A13S5-3 for $P>P_C$. Therefore, it seems that for the composites the liquid phase filled nearly completely the inter-fiber agglomerate- voids also activating the load transference mechanisms between heterogeneous fiber zones and matrix.

4.4.1. Unreinforced matrices for $P<P_C$

It is clear the Al–Cu reaction takes place already in the lower level of pressure during the ramp of pressure stage. QC experiments showed the extensive liquid flow between Al particles without any external pressure. During lower pressures in hot pressing, the presence of transient liquid phase enhances the relative movement between Al particles. That is to say, the rearrangement of particles, the consecutive plastic deformation, and finally, the densification of the whole porous material would be improved. In terms of strength the yield stress should decrease as compared to aluminum without liquid phase. When the densification of Alumix 13 for $P<P_C$ is compared with pure Al (AS081), using the same Konopicky plot, a clear-cut is made. Fig. 10a shows the decrease of Alumix 13 slope when the straight line belonging to AS081 is shifted (shaded line) for comparative purpose to Alumix 13 Konopicky plot. The A13-3 (610 °C) slope is 1.75 times lower than AS081 up to 7 MPa (Table 2), and it must be also noted that AS081 was hot pressed at a temperature 20 °C higher than that for A13-3. To reach those 7 MPa at least 50 s are needed, thus allowing the Al–Cu reaction followed by the liquid flow. Considering that AS081 and Alumix 13 aluminum particles are similar (both obtained by atomization, with the same Al purity) no other mechanism induces the softening of Al particles belonging to Alumix 13. Therefore, it can be said that the Al–Cu liquid phase enhances the densification of Al particles during the hot pressing at lower pressures. The quantity of present liquid depends on Al [22] and Cu particles sizes and temperature [4].

4.4.2. Unreinforced matrices for $P>P_C$

The second result from QC experiments was the rapid Cu diffusion into the Al matrix, which reduces the Cu content from the liquid phase. According to Fig. 9a, in A13-3 for pressures higher than P_C,

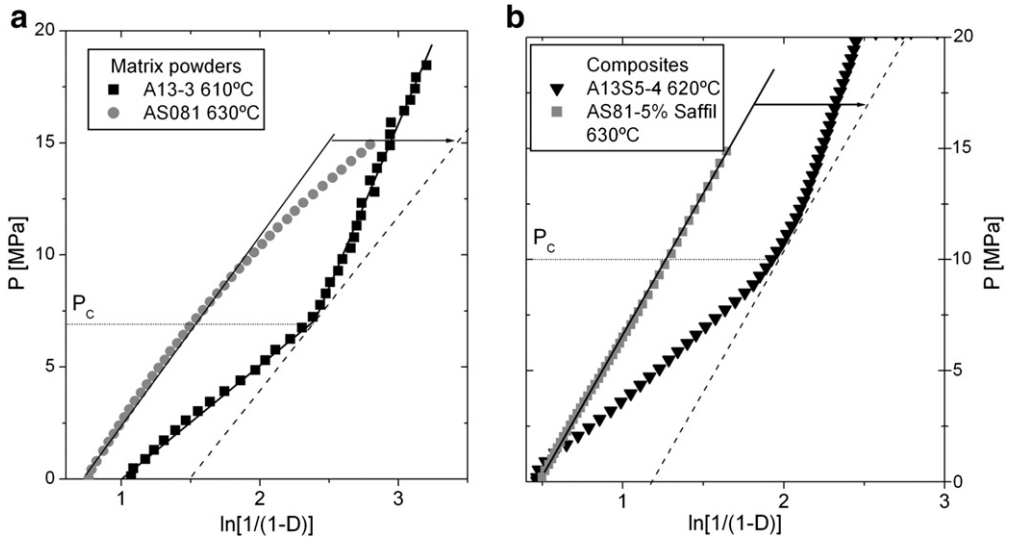

Fig. 9. Power Law Creep plots corresponding to Alumix 13 composites materials.

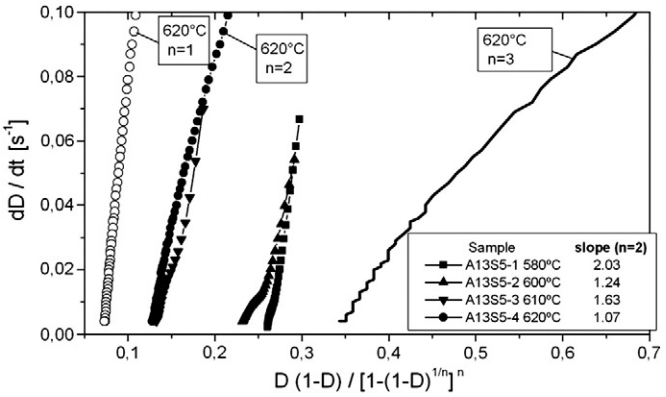

Fig. 10. Comparative Konopicky plots for a) pure matrices and b) composite materials.

the Al–Cu alloy is formed rapidly and an increase in the yield stress σ_{YS} is obtained (Table 2). This hardening behavior was evident, but the most important feature is that the straight linear Konopicky plot was maintained. Therefore, for pressures above P_C, Konopicky is still controlling the densification of the whole material. In summary, two processes take place during increasing pressure for the Alumix 13 powders because of the presence of the liquid phase: a softening before Pc and a hardening due to the rapid diffusion of Cu in the aluminum matrix for $P>P_C$.

It was assumed that the hardening is mainly due to alloy formation. This is easy to analyse when the same Konopicky plot again is compared with pure Al. Comparative hot pressing of pure AS081 at 630 °C (grey circles in Fig. 10a) resulted with lower yield stresses compared with that for A13-3. Furthermore, beyond 8 MPa for pure Al a clear softening behavior (negative curvature of Konopicky plot for AS081 in Fig. 10a) can be observed, opposite to the hardening showed by A13-3 material after the break slope.

4.4.3. Composites

Same previous Konopicky plots comparison can be done between composites materials based on different matrices: pure Al and Alumix13. Fig. 10b shows that a single straight slope is obtained during the ramp of pressure stage when composite AS081 with 5 wt.% Saffil is pressed at 630 °C. This slope equivalent to $\sigma_{YS} = 18.8$ MPa resulted double than 9.3 MPa (Table 2) corresponding to lower pressures σ_{YSI} for the composite A13S5-4. It is noteworthy that this softening of the Alumix composite happened at temperature 10 °C lower than for AS081 composite (630 °C). In similar way as for the unreinforced materials, for higher pressures than P_C the hardening developed by the A13S5-4 due to Cu diffusion into the Al, increased its slope to 1.7 times higher than for the pure Al composite. Therefore same behavior developed by Alumix 13 material is observed for the composites.

5. Conclusions

High density hot pressed samples at 580, 600 and 610 °C were obtained starting from mixture of elemental particles to give (wt.%) Al–4.5 Cu 0.5 Mg and 0.2 Si nominal composition (Alumix 13). Also 5 wt.% Saffil short fibers reinforced composites were hot pressed at 580, 600, 610 and 620 °C.

Konopicky plastic model allowed to fit the ramp of pressure stage densification of both materials: unreinforced matrix and composite. Such plots for the matrix at 610 °C gave two slopes (called 'behavior of changing slope' at $P = P_C$), steeper for pressures higher than P_C. That break in Konopicky plot means a hardening mechanism developing, which can be induced by the formation of solid solution due to the rapid Cu diffusion from liquid phase into the Al matrix grains. Also, this behavior of changing slope was observed systematically for the four composites.

In the hot pressings at pressures smaller than P_C, it seems that the formation and spreading of Al–Cu liquid phase enhances the densification for both materials: unreinforced metals and composites. That is, owing to the quick reaction between Al and Cu the transient liquid phase can work as lubricant improving the plastic deformation of Al particles, with or without presence of Saffil fibers. It was clear from Konopicky plots, that there were softening processes for Alumix 13 matrix for $P<P_C$ due to such liquid.

Using the Power Law Creep model the constant pressure stage for the composites could be well fitted using power exponents of $n = 1$ and $n = 2$, which are related to Newtonian viscous flow and superplastic densification mechanisms, respectively. Besides final hot pressed composites samples retained an important quantity of solidified liquid phase located in between the Saffil fibers agglomerates.

Acknowledgments

The authors gratefully acknowledge to C.O.N.I.C.E.T and A.N.P.C. y T. for financial supports. Facilities, equipments and technical support from the Groups División Física de Metales and Caracterización de Materiales, are also acknowledged, all belonging to Centro Atómico Bariloche, Comisión Nacional de Energía Atómica.

References

[1] Z.A. Munir, Surface oxides and sintering of metals, Powder Metallurgy 4 (1981) 177–180.
[2] W. Kehl, H.F. Fischmeister, Liquid phase sintering of Al–Cu compacts, Powder Metallurgy 23 (3) (1980) 113–119.
[3] G.B. Schaffer, T.B. Sercombe, R.N. Lumley, Liquid phase sintering of aluminium alloys, Materials Chemistry and Physics 67 (2001) 85–91.
[4] T.B. Sercombe, G.B. Schaffer, Effect of trace elements on the sintering of Al–Cu alloys, Acta Materialia 47 (1999) 689–697.
[5] S.W. Ip, M. Kucharski, J.M. Toguri, Wetting behaviour of aluminium and aluminium alloy on Al_2O_3 and CaO, Journal of Materials Science Letters 12 (1993) 1699–1702.
[6] M.L. Delgado, E.M. Ruiz-Navas, E. Gordo, J.M. Torralba, Enhancement of liquid phase sintering through Al–Si additions to Al–Cu systems, Journal of Materials Processing Technology 162–163 (2005) 280–285.
[7] M.F. Moreno, G. Urretavizcaya, C. González Oliver, Hot-pressing densification of Al (Al/Cu)-short Al_2O_3 fibres mixtures, Powder Metallurgy 43 (1) (2000) 83–88.
[8] Haar, J. Duszczyk, Mixing of powder metallurgical fibre-reinforced aluminum composites, Materials Science and Engineering 135 (1991) 65–72.
[9] M.F. Moreno, C.J.R. González Oliver, Densification of Al powder and Al–Cu matrix composite (reinforced with 15 wt.% Saffil short fibres) during axial cold compaction, Powder Technology (2010), http://dx.doi.org/10.1016/j.powtec.2010.09.034.
[10] C. Torre, Theorie und Verhalten der zusammengepreβten Pulver, Berg-Hüttenmänn. Monatsh. Montan. Hochschule Leoben, 93, 1948, pp. 62–67.
[11] Ogel, R. Gurbuz, Microstructural characterization and tensile properties of hot-pressed Al–SiC composites prepared from pure Al and Cu powders, Materials Science and Engineering 301A (2001) 213–220.
[12] M. F. Moreno, Sinterización e inyección metálica en compuestos de matriz metálica (MMC) de Al, Al–Cu y Al–Si: síntesis y comportamiento térmico y mecánico, PhD Thesis, (2009) Instituto Balseiro, Universidad Nacional de Cuyo, Argentina.
[13] M.F. Moreno, C.R.J. González Oliver, Compression creep of PM aluminum matrix composites reinforced with SiC short fibres, Materials Science and Engineering A 418 (1–2) (2006) 172–181, (25).
[14] D. S. Wilkinson, The mechanisms of pressure sintering, PhD Thesis, Cambridge University, Wolfson College, U.K., (1978) pp. 27.
[15] J. Harper, J.E. Dorn, Viscous creep of aluminum near its melting temperature, Acta Metallurgica 5 (1957) 654–665.
[16] R.S. Mishra, T.R. Bieler, A.K. Mukherjee, Overview No. 119: Superplasticity in powder metallurgy aluminum alloy and composites, Acta Metallurgica et Materialia 43 (3) (1995) 877–891.
[17] T.G. Nieh, J. Wadsworth, Superplasticity and superplastic forming of aluminum metal-matrix composites, Journal of Metals (1992) 46–50.
[18] M.J. Starink, A.M. Zahra, Mechanisms of combined GP zone and θ′ precipitation in an Al–Cu alloy, Journal of Materials Science Letters 16 (19) (1997) 1613–1615.
[19] A.P. Savitskii, Scientific approaches to problems of mixtures, Science of Sintering 37 (2005) 3–17.
[20] J.M. Martín, F. Castro, Liquid phase sintering of P/M aluminum alloys: effect of processing conditions, Journal of Materials Processing Technology 143–144 (2003) 814–821.
[21] J. Koike, M. Mabuchi, K. Higashi, In situ observation of partial melting in superplastic aluminum alloy composites at high temperatures, Acta Metallurgica et Materialia 43 (1995) 199–206.
[22] R.N. Lumley, G.B. Schaffer, The effect of solubility and particle size on the liquid phase sintering, Scripta Materialia 35 (5) (1996) 589–595.